5-5-2008

Close Encounters of Three Black Holes

Manuela Campanelli
Rochester Institute of Technology

Carlos O. Lousto
Rochester Institute of Technology

Yosef Zlochower
Rochester Institute of Technology

Recommended Citation

M. Campenelli, C.O. Lousto, and Y. Zlochower, Physical Review D 77, 101501 (2008). https://doi.org/10.1103/PhysRevD.77.101501

Close encounters of three black holes

Manuela Campanelli, Carlos O. Lousto, and Yosef Zlochower

Center for Computational Relativity and Gravitation,
School of Mathematical Sciences, Rochester Institute of Technology,
78 Lomb Memorial Drive, Rochester, New York 14623

(Dated: April 9, 2008)

We present the first fully relativistic longterm numerical evolutions of three equal-mass black holes in a system consisting of a third black hole in a close orbit about a black-hole binary. We find that these close-three-black-hole systems have very different merger dynamics from black-hole binaries. In particular, we see complex trajectories, a redistribution of energy that can impart substantial kicks to one of the holes, distinctive waveforms, and suppression of the emitted gravitational radiation. We evolve two such configurations and find very different behaviors. In one configuration the binary is quickly disrupted and the individual holes follow complicated trajectories and merge with the third hole in rapid succession, while in the other, the binary completes a half-orbit before the initial merger of one of the members with the third black hole, and the resulting two-black-hole system forms a highly elliptical, well separated binary that shows no significant inspiral for (at least) the first $t \sim 1000M$ of evolution.

PACS numbers: 04.25.Dm, 04.25.Nx, 04.30.Db, 04.70.Bw

Introduction: The recent dramatic breakthroughs in the numerical techniques to evolve black-hole-binary spacetimes [1, 2, 3] has led to rapid advancements in our understanding of black-hole physics. Notable among these advancements are developments in mathematical relativity, including systems of PDEs and gauge choices [4, 5, 6], the exploration of the cosmic censorship [7, 8, 9, 10, 11], and the application of isolated horizon formulae [8, 9, 12, 13, 14, 15]. These breakthroughs have also influenced the development of data analysis techniques through the matching of post-Newtonian to fully-numerical waveforms [16, 17, 18]. Similarly, the recent discovery of very large merger recoil kicks [19, 20, 21, 22, 23, 24, 25, 26] has had a great impact in the astrophysical community, with several groups now seeking for observational traces of such high speed holes as the byproduct of galaxy collisions [27, 28]. In this letter, we continue our quest to discover new astrophysical consequences of black-hole interactions by simulating close encounters of three black holes to see the different behaviors introduced by the finite size of the holes, their nonlinear interactions, and the radiation of gravitational waves, as described by General Relativity. We find that the three-body relativistic problem shows far richer dynamics than the two-body problem, akin to the rich three-body dynamics in Newtonian gravity, but with added complexity due to mergers.

Three-body and four-body interactions are expected to be common in globular clusters [29, 30], and in galactic cores hosting supermassive black holes (when stellar-mass-black-hole-binary systems interact with the Supermassive black hole). Hierarchical triplets of massive black holes might also be formed in galactic nuclei undergoing sequential mergers [31, 32]. The gravitational wave emission from such systems was recently estimated using post-Newtonian techniques [33].

Techniques: We evolve the three-black-hole data-sets using the LazEv [34] implementation of the 'moving puncture approach' [2, 3]. We use the Carpet [35] driver to provide a 'moving boxes' style mesh refinement. In this approach refined grids of fixed size are arranged about the coordinate centers of each hole. We use AHFinderDirect [36] to locate apparent horizons. We extract the waveform on spheres centered about the origin and extrapolate the radiated energy/momentum to $r = \infty$ (the waveforms do no change qualitatively for $r > 50 \pm 20M$).

Results: We chose one configuration (3BH1) with purely *ad-hoc* momentum parameters, which merged relatively quickly, to test the convergence and accuracy of our code. The initial data parameters for these configurations are summarized in Table I. We evolved these configuration using 11 levels of refinement and a finest resolution of $h = M/80$. The outer boundaries were located at $640M$. In addition we evolved the 3BH1 configuration with grid-spacings rescaled by 5/6 and $(5/6)^2$ to test convergence. In the table, the horizon mass is the Christodoulou mass, where $m^H = \sqrt{m_{\rm irr}^2 + S^2/(4m_{\rm irr}^2)}$, S is the magnitude of the spin of the hole, and $m_{\rm irr}$ is the irreducible mass.

It is interesting to note that the same techniques used for black-hole binary evolutions work for configurations of three (and, according to a brief test by the authors, at least 22) black holes. We tested the convergence of our algorithm with three black holes by evolving configuration 3BH1 with three resolutions $(M/80, M/96, M/115.2)$. We chose this configuration since it merges relatively quickly, thus reducing the computational expense. The resulting waveform converges to fourth-order. Note that late-time accumulation of errors can have a significant effect on the trajectories of 3-black-hole systems due to

TABLE I: Initial data parameters. $(x_i, y_i, 0)$ and $(p_i^x, p_i^y, 0)$ are the initial position and momentum of the puncture i, m_i^p is the puncture mass parameter, and m_i^H is the horizon mass.

Config	3BH1	3BH101	3BH102
x_1/M	-2.40856	-3.52462	-3.52238
y_1/M	2.23413	2.58509	2.58509
p_1^x/M	-0.0460284	-0.0782693	0.0782693
p_1^y/M	-0.0126181	-0.0400799	-0.0433529
m_1^p/M	0.315269	0.318143	0.317578
m_1^H/M	0.335555	0.336201	0.335721
x_2/M	-2.40856	-3.52462	-3.52462
y_2/M	-2.10534	-2.58509	-2.58509
p_2^x/M	0.130726	0.0782693	-0.0782693
p_2^y/M	-0.0126181	-0.0400799	-0.0433529
m_2^p/M	0.315269	0.318143	0.317578
m_2^H/M	0.3405205	0.336241	0.335767
x_3/M	4.8735	7.04923	7.04476
y_3/M	0.0643941	0	0
p_3^x/M	-0.0846974	0	0
p_3^y/M	0.0252361	0.0801597	0.0867057
m_3^p/M	0.315269	0.320815	0.318585
m_3^H/M	0.332198	0.333115	0.331270

their inherent sensitivity to changes in configuration. We have confirmed, through the use of a 8th-order accurate code, that the trajectories presented here show the correct qualitative behavior.

We now show results for two similar initial configurations with qualitatively different outcomes. To aid in the discussion, we will denote the two holes in the binary with BH1 and BH2, and the third hole with BH3, where BH1 is initially located at $y > 0$. We determined our initial data parameters by choosing a fiducial binary configuration with orbital frequency $M_B\Omega_B = 0.04$ and angular momentum $J_B/M_B^2 = 0.9104975$. We then treat the binary as a point particle of mass $M_B = 2/3M$ and spin $a_B/M_B = 0.9105$ along with a non-spinning point particle of mass $M/3$, and choose position and momenta parameters such that this two particle system is in a quasi-circular orbit (up to 3 PN) at a separation equal to twice the binary's separation. We set up the systems so that the binary's orbital angular momentum is aligned with the total orbital angular momentum (configuration 3BH101), and anti-aligned (configuration 3BH102). Configuration 3BH101 has BH2 and BH3 merging after the binary completes nearly a half of an orbit. The result of this interaction is to significantly push BH1 away from the merger remnant, producing a new, highly elliptical, binary, with large orbital separation oscillating in time from $10.4M$ to $23.5M$ (see Fig. 1). The 3BH101 waveform (Fig. 2) shows a burst of radiation from the BH2–BH3 merger, as well as a small pulse at $t \sim 700M$ which corresponds to the point of closest approach of the BH2–BH3 merger remnant with BH1. We stopped the evolution at $t \sim 1000M$ due to computational expense and boundary contamination.

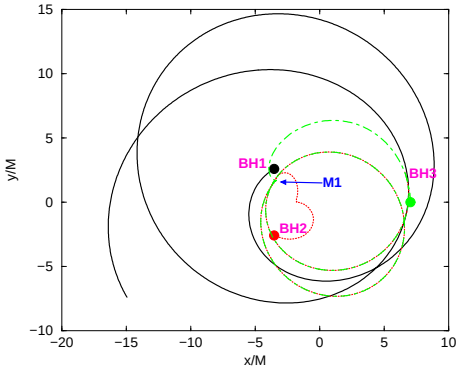

FIG. 1: The horizon trajectories for configuration 3BH101. The three black holes are initially located at the points labeled by BH1, BH2, and BH3, respectively. BH1 and BH2 form a quasi-circular binary, which is disrupted by BH3. BH2 and BH3 merge at point M1. The BH1 and the BH2–BH3 merger remnant continue to orbit each other throughout the simulation.

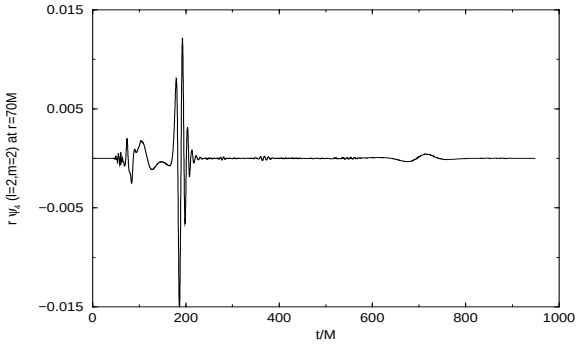

FIG. 2: The $(l = 2, m = 2)$ mode of ψ_4 for 3BH101. The BH2–BH3 merger waveform is centered at $t \sim 185M$, the small pulse at $t \sim 700$ was produced by the close approach of the BH2–BH3 merger product to BH1.

Configuration 3BH102 displays very different behavior, as seen in Fig. 3. Here the binary is disrupted almost immediately, and the individual holes follow complicated trajectories (note that the trajectories are similar to the Greek letters γ, τ, and σ). BH3 and BH1 merge when BH3 almost completes 1.25 orbits. The BH3–BH1 merger product then quickly merges with BH2. The resulting waveform shows a double merger as seen in Fig. 4. It is important to note that the dramatic difference in dynamics between 3BH101 and 3BH102 is not strictly due to corotation versus anti-corotation of the binary, but rather is a result the precise configuration of the binary when the third black hole approaches.

For all three configurations the radiated energy and angular momenta were a fraction of that for a quasi-circular equal-mass binary. This is due to the grazing type mergers, as also seen by the suppression of the radiated an-

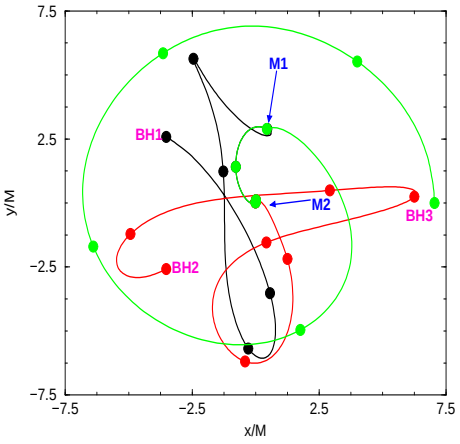

FIG. 3: The horizon trajectories for configuration 3BH102 with ticks every $45M$ of evolution. The three black holes are initially located at the points labeled BH1, BH2, and BH3, respectively. BH1 and BH2 form a quasi-circular binary, which is almost immediately disrupted by BH3. BH1 and BH3 merge at point M1, and then merge with BH2 at M2.

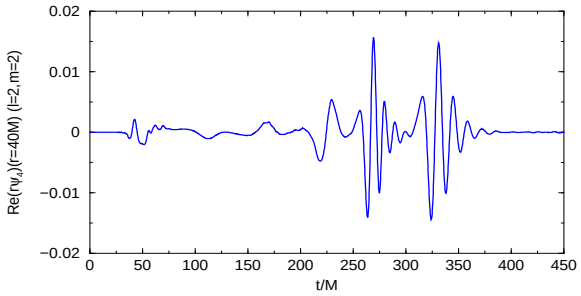

FIG. 4: The $(\ell = 2, m = 2)$ mode of ψ_4 for 3BH102 shows two merger waveform signals arising from merger M1 and M2.

gular momentum. We expect that the full waveform for 3BH101 will show significantly more radiation as the system eventually 'circularizes' and merges.

We calculate the mass and spin of the first merger remnant and the final remnant using the fitted exponential decay rate and frequency of the quasi-normal behavior [37]. For 3BH102, we fit the real and imaginary parts of the $(\ell = 2, m = 2)$ mode separately and find $a_H/M_H = 0.479, 0.378$ and $M_H = 0.716, 0.678$ from fits of the real and imaginary parts of ψ_4 for the first merger product, and $a_H/M_H = 0.478, 0.580$ and $M_H = 0.994, 1.04$ from fits of the real and imaginary parts of ψ_4 for the final merger remnant. Note that the imaginary part of ψ_4 provides a better estimate (i.e. closer to the expected 0.66) mass for the first remnant, but the real part provides a better estimate of both a and M_H for the final remnant. We note the quasi-normal frequencies were $\omega = 0.64, 0.46$ for the first and final merger remnants respectively. For

TABLE II: Total radiated energy, momentum, and angular momentum, as well as horizon mass spin and merger time, for 3BH102 and 3BH1. ($*$ 3BH101 did not merge in the time alloted and we only report values for the first merger).

Config	3BH1	3BH101*	3BH102
$E_{\rm rad}/M(\times 1000)$	6.06 ± 0.02	4.4 ± 0.8	6.1 ± 0.7
$J^z_{\rm rad}/M^2(\times 100)$	2.92 ± 0.01	3.6 ± 0.5	4.4 ± 0.2
$P^x_{\rm rad}/M({\rm km\,s^{-1}})$	20.0 ± 1.9	50 ± 40	-1.3 ± 14
$P^y_{\rm rad}/M({\rm km\,s^{-1}})$	-22.9 ± 2.4	27 ± 13	-15 ± 13
$M_{\rm H}/M$	0.9835	***	0.9885
$S^z_{\rm H}/M^2$	0.532	***	0.465
$t_{\rm M1}/M$	~ 27	~ 115	~ 218
$t_{\rm M2}/M$	~ 40	***	~ 280

3BH101 we were only able to fit the real part of ψ_4 due to significant contamination from other modes in the imaginary part. We find a narrow region of width $10M$ where the waveform shows nearly exponential decay. A fit to this region yields $\omega = 0.63$, with a corresponding mass and spin of $M_H = 0.665$ and $a/M_H = 0.293$. The remnant masses, spins, and merger times are given in Table II for the 3BH1 and 3BH102 configurations. The numbers quoted above should be taken only as indicative of the expected values of these parameters. Further runs, at higher resolutions, will be needed in order to establish the errors in these values.

Discussion: The relativistic study of quasi-circular orbits of a binary in the presence of a third comparable-mass hole, as an initial value problem, was studied in [38]. Here, by studying their dynamical evolution we find that the third hole perturbs the system to the extent that no true binary orbit is seen. We found that the close encounter of this third body can both trigger a quick merger of the three-body system, as well as impart a significant kick to one of the holes, producing a new long-lived, highly-elliptical binary. The generic effect of the third black hole is to reduce the gravitational radiation. This happens for two reasons. First, close-three-body interactions lead to grazing collisions, which emit far less radiation than quasi-circular mergers. Second, the resulting binary orbit will be elliptical, which is less efficient at emitting gravitational radiation than circular orbits at the final stages. Note however, that although we report radiated energies that are $1/5^{\rm th}$ that for a typical binary, here we scale the energy by the total mass. If we scale the radiated energy with the initial binary's mass, then the rescaled radiated energy would be 3/2 times larger. The close-three-body systems also appear to be shorter lived than typical binaries.

The three-black-hole waveforms (See Figs. 2 and 4) are distinct from the robust and simple form of the binary-black-hole waveform [39, 40, 41, 42]. In addition, there seems to be a large exchange of energy among the components of the triple system, which occurs on a much shorter timescale than the radiation. It is important to

note that these three-black-hole interactions provide a mechanism for producing highly-elliptical close-binaries, which would otherwise have circularized (due to emission of gravitational radiation during the inspiral).

Investigations of the Newtonian encounters of three bodies show that such encounters generically lead to the breakup of the system into a binary and the third body that escapes [43] in a 'water-shed effect'. The distribution of the eccentricity of the remaining binary is bell shaped around $e = 0.3$ for compact systems [44, 45]. Classical studies [46] show that the probability of exchange of the binary companion in a triple system is surprisingly high for all comparable masses, reaching near one for more massive m_3 [47]. The motion of the system can be chaotic, due to small denominators. The finite size of the black holes represents a natural regularization to the problem, and the dissipative effects of the gravitational radiation can prevent some configurations from becoming chaotic.

We have found that 3-black-hole systems exhibit complicated orbital dynamics analogous to the rich 3-body Newtonian dynamics, but with the added complexity introduced by mergers. Further study of this problem, including a comparison of Newtonian and relativistic dynamics, will be reported in a forthcoming paper, where we also examine configurations where the triple system is disrupted.

We thank Alessia Gualandris, David Merritt, and Hiroyki Nakano for valuable discussions. We gratefully acknowledge NSF for financial support from grant PHY-0722315, PHY-0701566, PHY 0714388, and PHY 0722703; and NASA for financial support from grant NASA 07-ATFP07-0158. We also thank Hans-Peter Bischof for producing 3-D visualizations of the three-black-hole configurations introduced in this paper. Computational resources were provided by the NewHorizons cluster at RIT and the Lonestar cluster at TACC.

[1] F. Pretorius, Phys. Rev. Lett. **95**, 121101 (2005).
[2] M. Campanelli, C. O. Lousto, P. Marronetti, and Y. Zlochower, Phys. Rev. Lett. **96**, 111101 (2006).
[3] J. G. Baker, J. Centrella, D.-I. Choi, M. Koppitz, and J. van Meter, Phys. Rev. Lett. **96**, 111102 (2006).
[4] C. Gundlach and J. M. Martin-Garcia, Phys. Rev. **D74**, 024016 (2006).
[5] J. R. van Meter, J. G. Baker, M. Koppitz, and D.-I. Choi, Phys. Rev. **D73**, 124011 (2006).
[6] L. Lindblom, M. A. Scheel, L. E. Kidder, R. Owen, and O. Rinne, Class. Quant. Grav. **23**, S447 (2006).
[7] M. Campanelli, C. O. Lousto, and Y. Zlochower, Phys. Rev. D **74**, 041501(R) (2006).
[8] M. Campanelli, C. O. Lousto, and Y. Zlochower, Phys. Rev. D **74**, 084023 (2006).
[9] M. Campanelli, C. O. Lousto, Y. Zlochower, B. Krishnan, and D. Merritt, Phys. Rev. **D75**, 064030 (2007).
[10] L. Rezzolla et al. (2007), arXiv:0710.3345 [gr-qc].
[11] U. Sperhake et al. (2007), arXiv:0710.3823 [gr-qc].
[12] B. Krishnan, C. O. Lousto, and Y. Zlochower, Phys. Rev. **D76**, 081501 (2007).
[13] O. Dreyer, B. Krishnan, D. Shoemaker, and E. Schnetter, Phys. Rev. **D67**, 024018 (2003).
[14] E. Schnetter, B. Krishnan, and F. Beyer, Phys. Rev. **D74**, 024028 (2006).
[15] A. Ashtekar, S. Fairhurst, and B. Krishnan, Phys. Rev. **D62**, 104025 (2000).
[16] Y. Pan et al. (2007), arXiv:0704.1964 [gr-qc].
[17] M. Boyle et al. (2007), arXiv:0710.0158 [gr-qc].
[18] M. Hannam, S. Husa, U. Sperhake, B. Brugmann, and J. A. Gonzalez (2007), arXiv:0706.1305 [gr-qc].
[19] M. Campanelli, C. O. Lousto, Y. Zlochower, and D. Merritt, Astrophys. J. **659**, L5 (2007).
[20] J. A. Gonzalez, M. D. Hannam, U. Sperhake, B. Brugmann, and S. Husa, Phys. Rev. Lett. **98**, 231101 (2007).
[21] M. Campanelli, C. O. Lousto, Y. Zlochower, and D. Merritt, Phys. Rev. Lett. **98**, 231102 (2007).
[22] F. Herrmann, I. Hinder, D. Shoemaker, P. Laguna, and R. A. Matzner (2007), gr-qc/0701143.
[23] M. Koppitz et al., Phys. Rev. Lett. **99**, 041102 (2007).
[24] J. G. Baker et al., Astrophys. J. **653**, L93 (2006).
[25] F. Herrmann, D. Shoemaker, and P. Laguna (2006), gr-qc/0601026.
[26] J. A. Gonzalez, U. Sperhake, B. Bruegmann, M. Hannam, and S. Husa, Phys. Rev. Lett. **98**, 091101 (2007).
[27] E. W. Bonning, G. A. Shields, and S. Salviander (2007), arXiv:0705.4263 [astro-ph].
[28] K. Holley-Bockelmann, K. Gultekin, D. Shoemaker, and N. Yunes (0700), arXiv:0707.1334 [astro-ph].
[29] K. Gultekin, M. C. Miller, and D. P. Hamilton, AIP Conf. Proc. **686**, 135 (2003).
[30] M. C. Miller and D. P. Hamilton (2002), astro-ph/0202298.
[31] M. J. Valtonen, MNRAS **278**, 186 (1996).
[32] J.-c. Makino and P. Hut, Astrophys. J. **365**, 208 (1990).
[33] K. Gultekin, M. Coleman Miller, and D. P. Hamilton, Astrophys. J. **640**, 156 (2006).
[34] Y. Zlochower, J. G. Baker, M. Campanelli, and C. O. Lousto, Phys. Rev. D **72**, 024021 (2005).
[35] E. Schnetter, S. H. Hawley, and I. Hawke, Class. Quantum Grav. **21**, 1465 (2004).
[36] J. Thornburg, Class. Quantum Grav. **21**, 743 (2004).
[37] F. Echeverría, Phys. Rev. D **40**, 3194 (1989).
[38] M. Campanelli, M. Dettwyler, M. Hannam, and C. O. Lousto, Phys. Rev. **D74**, 087503 (2006).
[39] J. Baker, B. Brügmann, M. Campanelli, C. O. Lousto, and R. Takahashi, Phys. Rev. Lett. **87**, 121103 (2001).
[40] J. Baker, M. Campanelli, C. O. Lousto, and R. Takahashi, Phys. Rev. D **65**, 124012 (2002).
[41] M. Campanelli, C. O. Lousto, and Y. Zlochower, Phys. Rev. D **73**, 061501(R) (2006).
[42] J. G. Baker, J. Centrella, D.-I. Choi, M. Koppitz, and J. van Meter, Phys. Rev. D **73**, 104002 (2006).
[43] J. J. Monaghan, MNRAS **176**, 63 (1976).
[44] P. Kroupa, MNRAS **277**, 1491 (1995).
[45] A. Duquennoy and M. Mayor, Astron. Astrophys. **248**, 485 (1991).
[46] J. G. Hills, Astron. J. **80**, 809 (1975).
[47] S. Sigurdsson and E. S. Phinney, Astrophys. J. **415**, 631 (1993).